Proc. Natl. Acad. Sci. USA
Vol. 92, pp. 180–184, January 1995
Biochemistry

Stereoelectronic effects of deoxyribose O4′ on DNA conformation

(ribose–base stacking/C—H···O hydrogen bonds/stereoelectronic effect/sequence dependence of DNA conformation/short O···C=N$^+$ contacts)

MARTIN EGLI†‡ AND REINHARD V. GESSNER§

†Organic Chemistry Laboratory, Swiss Federal Institute of Technology, CH-8092 Zürich, Switzerland; and §Institute for Clinical Chemistry and Biochemistry, Rudolf Virchow University Hospital, D-14050 Berlin, Germany

Communicated by Jack D. Dunitz, Eidgenössische Technische Hochschule, Zürich, Switzerland, August 25, 1994

ABSTRACT **While B-DNA, the most common DNA conformation, displays rather regular twist angles and base stacking between successive base pairs, left-handed Z-DNA is characterized by the alternation of two different dinucleotide conformations with either a large twist and a small slide or a small twist and a large slide between adjacent base pairs. This results in poor stacking within the latter dinucleotide repeat that is in apparent contradiction to the rigidity and conformational stability of Z-DNA at high ionic strength. However, at d(CpG) steps the cytidine deoxyribose is situated such that its O4′ sits directly over the six-membered ring of the guanine. We show here that the particular positionings of the two O4′ lone-pair electrons provide stability through an intracytidine O4′···H6—C6 hydrogen bond and an $n \rightarrow \pi^*$ interaction with the guanidinium system of the stacked base. Our model is based on the assumption of a strong polarization of the guanine bases in Z-DNA that is consistent with the Z-DNA-specific guanine O6 and N7 coordination to metal and organic cations and the proximity of its N2 and C8 positions to neighboring phosphate groups, as well as several other Z-DNA-specific conformational features.**

In contrast to the influence of the ring oxygen on the reactivity and structural properties of the anomeric carbon center in pyranoses and furanoses, which has been investigated extensively (e.g., refs. 1–3), the structural consequences arising from the presence of the oxygen lone-pair electrons in the sugar framework of oligonucleotides have been discussed in much less detail. In double-stranded RNA fragments, ribose O4′ (sometimes termed O1′) can stabilize the A conformation by accepting a hydrogen bond from the 2′-hydroxyl group from the adjacent 5′-ribose (4, 5). In crystal structures of B-DNA dodecamers with sequences of the type CGCXXXXXXGCG (X is usually A or T), O4′ oxygens in the central region of the duplex stabilize the minor groove hydration spine via a series of hydrogen bonds (6). The stacking of several deoxyribose O4′ oxygens on the aromatic rings of the synthetic dye Hoechst 33258 seems to contribute significantly to the binding of the dye to the minor groove of B-DNA dodecamers (7–10). Stacking of a deoxyribose onto an adenine base with one of the oxygen lone pairs pointing into the base six-membered ring was also observed in the crystal structure of the cyclic 5′,3′-deoxydinucleotide ApAp (11).

The large slide for stacked bases at d(CpG) steps in Z-DNA with the resulting deoxyribose–base stacking can be noted in early illustrations of the Z duplex (12, 13) but was not specifically mentioned in descriptions of the structure. Three crystal structures of left-handed hexamers with sequence d(CGCGCG) were determined with particularly high precision. These are the original mixed spermine/magnesium form (12), the magnesium form (14, 15), and the pure-spermine form (16, 17). They were briefly reviewed in an earlier contribution, where their hydration was analyzed (18). Here, we describe details of the deoxyribose–base interactions at each of the total 18 d(CpG) steps in these structures and discuss the consequences in terms of stability and sequence dependence of Z-DNA. At d(CpG) steps the cytidine O4′ oxygen is situated above the six-membered ring of guanine (Fig. 1). Whereas the average helical rise at d(GpC) steps is ≈3.4 Å on average, it is about 4 Å at d(CpG) steps, at first sight suggesting a decrease in total stacking energy at such steps. However, closer examination of the orientation of the O4′ lone pairs and the resulting interactions within the nucleoside as well as with the stacked base suggest that the unusual deoxyribose–base interaction may be a significant stabilizing factor in Z-DNA that could possibly compensate for the lack of efficient base–base stacking at every second step.

METHODS

To assess the close contacts between O4′ and C6 within cytidine residues and between O4′ and the adjacent base plane of the stacked guanine at d(CpG) steps, the geometries of ring carbon atom C6 and O4′ were assumed to be that of ideal sp^2- and sp^3-hybrids, respectively (Fig. 2). The positions of hydrogen atoms H6 were calculated assuming a C6—H6 bond length of 1 Å. To differentiate between the two O4′ lone pairs, the one pointing to the same side of the furanose ring as the glycosidic bond is called β and the other one α. In the Z-DNA duplex, cytosine O4′ lone pairs α point roughly along the helix axis, whereas lone pairs β point roughly perpendicular to the helix axis (Figs. 1 and 2). To calculate the geometries of interactions, the vectors describing the direction of the β lone pairs (see Table 1) and the α lone pairs (see Table 2) were both assigned a hypothetical length of 1 Å. To compare the positions of deoxyriboses relative to the guanine base in the crystal structures, guanine base atoms (including C1′) from all steps were superimposed. Similarly, the ionic environment around guanine C8 was generated by separately analyzing the surrounding groups in the three structures and then superimposing the guanine bases.

RESULTS AND DISCUSSION

The Intracytidine C6—H6···O4′ Hydrogen Bond. Whereas the glycosidic torsion angles in right-handed B-DNA double helices cover a considerable range, the variations for A-DNA double helices and the left-handed Z-DNA double helix are more limited, consistent with the larger overall conformational rigidity of the latter two duplex types. Fig. 3 depicts the correlation between torsion angle O4′—C1′—N1—C6 (χ + 180° approximately) and the distance O4′···C6 for cytidine residues in the three duplex types. The included B-DNA duplexes are [d(CGCGAATTCGCG)]$_2$ [low-temperature (16

The publication costs of this article were defrayed in part by page charge payment. This article must therefore be hereby marked "*advertisement*" in accordance with 18 U.S.C. §1734 solely to indicate this fact.

‡To whom reprint requests should be addressed.

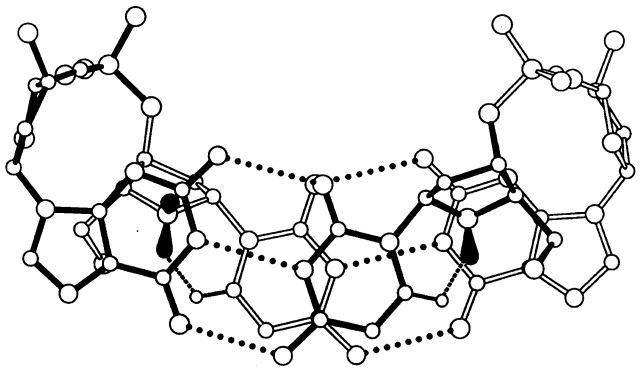

FIG. 1. Stacking interactions at d(CpG) steps in Z-DNA duplexes, viewed approximately along the helix axis. The small helical twist (−7° to −12°) together with the large slide (5.0 Å to 5.4 Å) results in only weak interstrand stacking between cytidine residues and places their deoxyriboses above the six-membered rings of adjacent guanine bases. The top base pair is drawn with solid bonds, Watson–Crick hydrogen bonds are dotted lines, C6—H6 bonds of cytosine are drawn with reduced radii, O4′ lone pairs are filled, and C6—H6···O4′ hydrogen bonds are dashed lines.

K) structure, NDB (nucleic acid data base) code BDL002 (19)], [d(GCGCGC)]$_2$ (BDFP24), [d(CGATCGATCG)]$_2$ (BDJB48), and [d(CCAGGCCTGG)]$_2$ (BDJB27). The included A-DNA duplexes are [d(CCCCGGGG)]$_2$ (ADH012), [d(ACCGGCCGGT)]$_2$ (ADJ022), and [d(CCCCCGCGGGGG)]$_2$ (ADL025). Small torsion angles as an expression of nearly eclipsed arrangements of the C1′—O4′ and N1—C6 bonds are associated with short 1···4 contacts between O4′ and C6 of around 2.6 Å. In contrast to the normally staggered conformation around C1′—N1 in the case of B-DNAs [except for certain cytidine residues in the first B-DNA single crystal structure (20)], A-DNA and Z-DNA are associated with tight O4′···C6 contacts. No significant deviations from the pattern observed for the d(CG)$_3$ duplexes are found in the crystal structures of [d(*CGTA*CG)]$_2$ [*C = 5-meC or 5-brC (21)] and [d(brCGATbrCG)]$_2$ (22). In A-DNA, puckers are usually of the C3′-*endo* type, whereas cytidine residues in Z-DNA adopt C2′-*endo* pucker. Although the directionalities between the O4′ lone pair and C6—H6 bond vary slightly for cytidine residues in A-DNA, a close O4′···C6 contact is maintained in all of them. The C6—H6···O4′ hydrogen bond should therefore also provide stability in A-type RNA duplexes.

In the three Z-DNA hexamers, the average value for torsion angle O4′—C1′—N1—C6 is 27° (maximum, 36°; minimum,

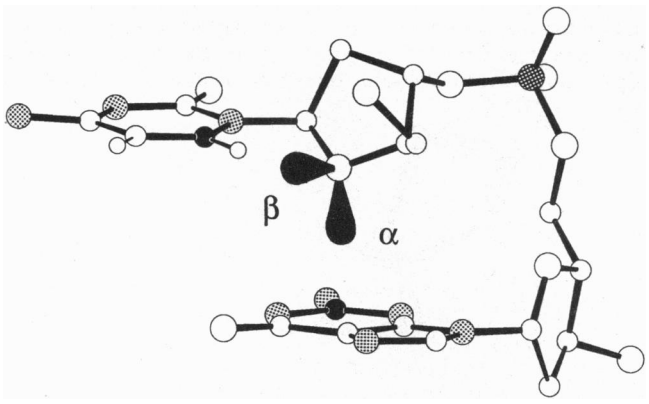

FIG. 2. An isolated d(CpG) base step viewed approximately normal to the helix axis. The β lone pair of O4′ and the cytosine base plane are nearly coplanar, and the α lone pair is nearly normal to the plane defined by the stacked guanine base. The positions of cytosine hydrogen atoms were calculated and lone pairs are filled. The phosphorus is crosshatched, nitrogens are stippled, and the C2 and C6 carbons of guanine and cytosine, respectively, are filled.

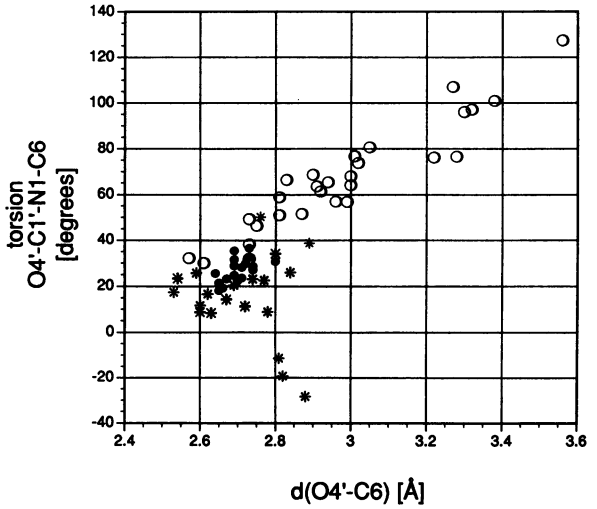

FIG. 3. Correlation between torsion angles O4′—C1′—N1—C6 (χ + 180°) and intracytidine O4′···C6 distances [d(O4′-C6)] for selected A-DNA (*, see text), B-DNA (○), and three Z-DNA duplexes (●). For equal bond lengths (1.4 Å) and equal bond angles (115°), the relationship between O4′···C6 distance (d_{14}) and torsion angle (ω) is $d_{14} = (9.90 - 3.32 \cos \omega)^{1/2}$.

18°) corresponding to a short O4′···C6 contact of around 2.7 Å and to a value for angle O4′···H6—C6 of ≈100° (Table 1). Thus, the intracytidine C—H···O distance is in a range associated with C—H···O hydrogen bonding (23, 24). The β lone pairs of O4′ oxygens lie roughly in the planes defined by cytosine bases with angles between lone pair and C6—H6 directions of around 110° (Figs. 1 and 2). However, C—H···O type hydrogen bonds are considerably less linear compared with O—H···O hydrogen bonds (mean, 153°; ref. 24). In 13 examples of C—H···O hydrogen bonds with nucleoside and nucleotide crystal structures, the O···H distance was <2.55 Å, with C—H···O angles between 103° and 171° (25). In 10 of these cases, the hydrogen bonds were to strong acceptor groups such as P═O and C═O, and interestingly, in 8 examples of three-center hydrogen bonds with O···H distances between 2.17 Å and 2.55 Å, the dominant donor was C6—H of pyrimidines. It appears therefore that the close C6—H6···O4′ contact can stabilize the Z-DNA conformation with d(CG)$_3$-type duplexes, probably due to a $n_{O4'} \rightarrow \sigma^*_{C6H}$ hyperconjugative effect.

Table 1. The cytidine O4′···C6 interaction

Parameter	O4′-C6	O4′-H6	lp β-H6	O4′-H6-C6	lp β-H6-C6	O4′-lp β-H6
Mixed spermine/magnesium form						
Max.	2.73	2.45	1.64	99.3	113.8	144.9
Min.	2.65	2.30	1.41	94.5	105.6	135.3
Avg.	2.70	2.39	1.53	97.0	110.3	140.6
σ	0.02	0.05	0.07	1.8	3.1	3.0
Magnesium form						
Max.	2.74	2.44	1.59	99.3	115.5	145.8
Min.	2.64	2.33	1.45	96.2	109.0	138.7
Avg.	2.70	2.39	1.52	97.1	110.7	142.4
σ	0.03	0.04	0.05	1.1	2.2	2.5
Pure-spermine form						
Max.	2.80	2.48	1.65	101.2	116.2	144.0
Min.	2.65	2.27	1.38	94.7	109.0	134.9
Avg.	2.70	2.38	1.53	98.0	113.2	139.7
σ	0.05	0.08	0.10	1.9	2.2	3.1

Maximum, minimum, and average values of selected distances (in Å) and angles (in degrees) for 18 cytidine residues. lp β designates the endpoint of a calculated vector along the direction of the O4′ β lone pair with a hypothetical length of 1 Å.

Table 2. The O4′ (C)···C2 (G) interaction

Parameter	O4′-G*	lp α-G*	O4′-C2	lp α-C2	O4′-C2-N2	O4′-lp α-C2
Mixed spermine/magnesium form						
Max.	2.90	1.98	3.03	2.09	106.8	173.3
Min.	2.78	1.80	2.89	1.90	105.1	155.6
Avg.	2.86	1.91	2.98	2.00	105.7	168.1
σ	0.05	0.06	0.05	0.06	0.6	6.0
Magnesium form						
Max.	2.96	2.01	3.05	2.06	107.1	178.9
Min.	2.82	1.85	2.94	1.95	101.3	169.7
Avg.	2.89	1.93	3.01	2.02	105.1	173.2
σ	0.05	0.06	0.04	0.04	2.0	2.8
Pure-spermine form						
Max.	2.93	1.95	3.09	2.11	109.7	173.5
Min.	2.83	1.83	2.90	1.95	99.7	157.1
Avg.	2.87	1.90	2.99	2.02	103.8	164.5
σ	0.04	0.04	0.06	0.05	3.1	5.8

Maximum, minimum, and average values of selected distances (in Å) and angles (in degrees) for 18 CpG steps. lp α designates the endpoint of a calculated vector along the direction of the O4′ α lone pair with a hypothetical length of 1 Å. G* designates the best plane through guanine base atoms.

Chemical substitution such as methylation at the 5-position of cytosine affects the tendency of DNAs containing repeated d(CpG) sequences to adopt the left-handed Z-DNA conformation (26). Pyrimidine C5 substituents can exert their maximal effect only if present on both strands, and influences are practically equivalent for thymine and cytosine (27). Pyrimidine C5 substituents promote the B-DNA → Z-DNA transition in the following order of efficiency: iodo > bromo > methyl ≫ H (28). A·T base pairs destabilize Z-DNA, and crystal structures could be determined only for $[d(CGTACG)]_2$ duplexes with cytosine C5 positions methylated or brominated but not for the unmodified hexanucleotides (21) {interestingly, the unmodified decamer $[d(CGCGTACGCG)]_2$ spontaneously adopts a left-handed conformation in the crystal (unpublished data)}. However, compared with the methylated hexamer that forms crystals slowly, crystals of the brominated hexamer grow readily. This is consistent with a much stronger stabilization of the Z-conformation with 5-bromocytosine derivatives of poly(dG-dC)·poly(dG-dC) relative to the methylated polymer (28). It was suggested that stabilization of Z-DNA upon 5-methylation or 5-bromination of cytosine stems from a destabilization of B-DNA through distorting hydration in the major groove and favorable hydrophobic interactions of the C5 substituents on the convex surface of Z-DNA (29, 30). Electronically, the methyl group is a σ-donor, which will raise the pK of C6 while rendering N3 a stronger donor. Bromine should have the opposite effect. The differing stabilizing effects of the two substituents on Z-DNA formation can be discussed in terms of a modulation of the C6—H6···O4′ hydrogen bond strength: bromination would strengthen the hydrogen bond and methylation would weaken it, while both substituents would exert their influence primarily through a destabilization of B-DNA and a stabilization of the Z-form via lipophilic contacts.

The $n_{O4'} \rightarrow \pi^*_{C=N^+}$ Interaction Between Cytidine Deoxyribose and Guanine Base. The α lone pairs of cytidine O4′ point into the six-membered rings of adjacent guanine bases (Figs. 1 and 2). Geometrical details are given in Table 2, and a superposition of the orientation of the sugar portions of cytidine residues with respect to the guanine bases in the magnesium form of the hexamer d(CGCGCG) is shown in Fig. 4. The geometry of the deoxyribose–guanine interaction is highly conserved throughout all d(CpG) steps in the three Z-DNA crystal structures. A comparison of distances between O4′ and guanine base atoms reveals that the furanose oxygen is consistently closest to ring carbon C2. Although the average O4′···C2 distance is only slightly below the sum of the van der Waals radii for the two atoms, the relative arrangement of O4′ and the exocyclic C2—N2 bond is compatible with an $n \rightarrow \pi^*$ hyperconjugation that stabilizes the guanidinium system of the base (Table 2). The average O4′···C2—N2 angle of around 105° is close to that between the directions of the antibonding π^* orbital and an assumed C2=N2$^+$ imino bond (Figs. 4 and 5). Also, the angle O4′—lone pair α—C2 is almost linear and guarantees a strong hyperconjugative effect.

Interactions of this type were first studied with intra- and intermolecular O···C=O and N···C=O contacts in crystals in an attempt to map reaction coordinates for the addition of nucleophiles to the carbonyl group and the reverse process (31, 32). From this point of view, the O4′···C2 contact in Z-DNA can be regarded as a nucleophilic addition reaction frozen at an early stage. A more advanced stage of such a reaction occurs in the crystal structure of the enzyme creatinase (33, 34). There, the nucleophile is water, which transfers a proton to an adjacent histidine and then attacks the guanidinium carbon of creatine as OH^- to produce a tetrahedral intermediate. Delocalization of the positive charge on creatine is reduced by neighboring glutamic acid residues, which withdraw electron density from the guanidinium carbon. The high stability of the guanidinium ion would normally render the observed interaction only slightly favorable. However, coordination of hydrated magnesium ions or positively charged nitrogens of polyamines to N7 and/or O6 groups on the convex surface of Z-DNA duplexes could result in a destabilization of the guanidinium system through delocalization of electrons into the exocyclic C6=O6 carbonyl group. By taking the ionic environment into account, one may postulate a mesomeric

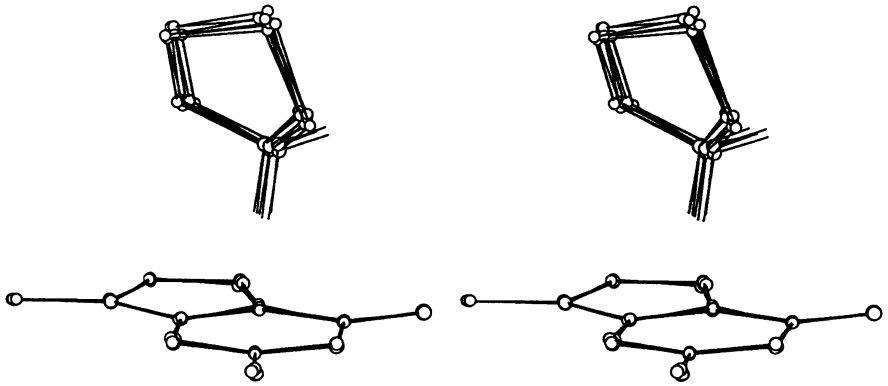

FIG. 4. Stereo drawing illustrating the high degree of conservation in the relative positionings of the cytidine deoxyribose and its 3′-adjacent guanine base at the six d(CpG) steps in the magnesium form of the Z-DNA hexamer d(CGCGCG). Only guanine base atoms were superimposed, and O4′ lone pairs are thin lines.

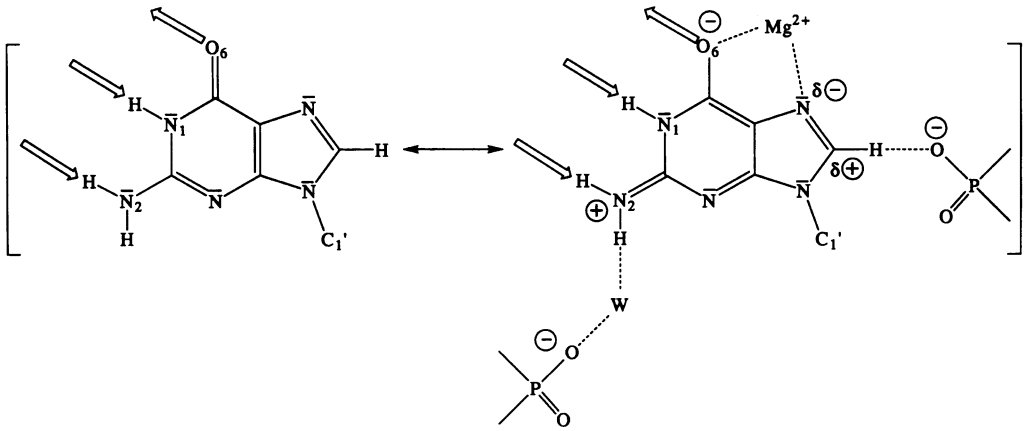

FIG. 5. Standard guanine (*Left*) and representative mesomeric form for guanine in Z-DNA duplexes $[d(CGCGCG)]_2$ (*Right*). Atoms participating in Watson–Crick hydrogen bonds are numbered (see also Table 3).

form for guanine in Z-DNA, which is depicted in Fig. 5. Cation coordination to nitrogen N7 renders the C8 carbon atom more positive and lowers its pK. The presence of negatively charged phosphate oxygens from neighboring duplexes at distances of <4 Å around C8 in 10 out of 18 cases in the three Z-DNA crystal structures provides convincing evidence for the increased acidity of C8. In addition to hydrogen bonds to phosphates, the analysis of C8 environments reveals hydrogen bonds to water molecules as well as to terminal O3′ and O5′ oxygen atoms from neighboring duplexes in 10 cases (upper distance limit 3.5 Å). The superimposed C8 environments are shown in Fig. 6.

Replacement of a G·C by an A·T base pair in a stretch of alternating d(G-C) will still result in a close deoxyribose (C)···A contact but cannot stabilize the Z conformation in the same way as the O4′ (C)···G interaction. The average distance between O4′ and adenine base planes in the $[d(CGTACG)]_2$ Z-DNA duplex is about 0.15 Å longer than that one between O4′ and guanine in the $[d(CGCGCG)]_2$ duplexes. Further support for a stabilizing effect of the interaction between O4′ and the assumed C2=$N2^+$ (G) bond comes from the fact that the average O4′ (T)···C2 (A) distance in the $[d(CGTACG)]_2$ duplex is more than 0.25 Å longer than the corresponding average O4′ (C)···C2 (G) distance in the $d(CG)_3$-type duplexes (3.26 Å and 3.22 Å, respectively). However, incorporation of A·T base pairs with conservation of an alternating purine-pyrimidine arrangement still allows formation of intra-pyrimidine C6—H6···O4′ hydrogen bonds, whereas out-of-alternation incorporation as in $[d(*CGAT*CG)]_2$ duplexes [*C = 5-brC or 5-meC (22)] leads to loss of the stabilizing deoxyribose–base contact, requires the energetically disfavored *syn* conformation for pyrimidines, and thus also prevents formation of C6—H6···O4′ hydrogen bonds.

Our hypothesis that the electronic state of G in Z-DNA differs from the one in A- and B-DNA is also supported by geometrical differences of G·C base pairs in left-handed and right-handed duplexes (Table 3). Comparison of G·C geometries in the three Z-DNA hexamers and in two of the most precise right-handed duplexes {A-RNA $[r(GC)]_2$ (NDB code ARB004) and B-DNA $[d(CCAACGTTGG)]_2$ (NDB code BDJ019)} shows that in Z-DNA the N2···O2 hydrogen bonds in the minor groove are somewhat longer on average compared with the O6···N4 hydrogen bonds in the convex surface, with an opposite situation in the right-handed duplexes. Is the slight opening-up of the G·C base pair in the minor groove of Z-DNA a consequence of the repulsion between negatively charged phosphate groups that are closely spaced across the minor groove in the left-handed duplex? For Z-DNA, the average C1′···C1′ distances are about 0.1–0.2 Å longer than the corresponding distances in the right-handed duplexes (Table 3). In the pure-spermine form, the negatively charged phosphate groups are shielded by the positively charged spermine in the minor groove (17). However, the average C1′···C1′ distance in that form is still slightly longer than the corresponding distance in the B-DNA decamer. It is therefore reasonable to attribute part of the difference in C1′···C1′ distances between left- and right-handed duplexes to the altered polarization of guanine in Z-DNA. Accordingly, the negative polarization of the guanine O6 keto oxygen in the convex surface of Z-DNA would strengthen the O6···N4 hydrogen bond, whereas the positive polarization of the guanine N2 nitrogen in the minor groove would weaken the N2···O2 hydrogen bond.

Conclusions. The stabilizing function attributed to cytidine O4′ in Z-DNA through contacts via its lone-pair electrons is consistent with the influences of base sequence and chemical

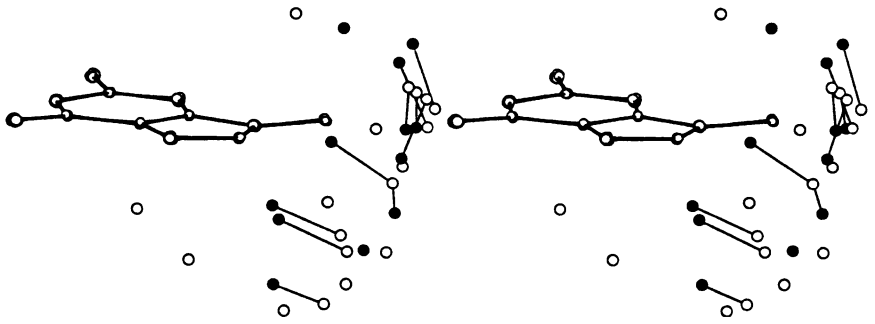

FIG. 6. Stereo drawing illustrating the environment around guanine C8 in the lattices of the three $[d(CGCGCG)]_2$ crystal forms. Phosphate oxygens located at a distance of up to 4 Å and uncharged hydrogen bond acceptors located at a distance of up to 3.5 Å around C8 were included. The overall environment was generated by superimposing totally 14 guanine bases. P (open circles) —O (filled circles) bonds are thin lines, O5′ and O3′ are isolated filled circles, and waters are isolated open circles.

Table 3. The geometry of G·C base pairs in A-, B-, and Z-type duplexes

	Guanine		Cytosine		Watson–Crick hydrogen bonds			Distance
Parameter	C6-O6	C2-N2	C4-N4	C2-O2	O6···N4	N1···N3	N2···O2	C1′···C1′
Mixed spermine/magnesium form								
Max.	1.28	1.32	1.36	1.25	2.89	2.95	2.93	10.89
Min.	1.23	1.28	1.32	1.22	2.80	2.89	2.85	10.78
Avg.	1.26	1.30	1.34	1.24	2.85	2.92	2.90	10.82
σ	0.02	0.02	0.02	0.01	0.04	0.02	0.03	0.04
Magnesium form								
Max.	1.27	1.31	1.37	1.25	2.91	2.98	2.95	10.86
Min.	1.25	1.27	1.35	1.22	2.81	2.91	2.82	10.78
Avg.	1.27	1.30	1.36	1.24	2.86	2.93	2.89	10.82
σ	0.01	0.01	0.02	0.01	0.03	0.03	0.04	0.03
Pure-spermine form								
Max.	1.29	1.32	1.41	1.25	2.87	2.96	2.93	10.82
Min.	1.24	1.25	1.32	1.20	2.79	2.87	2.86	10.66
Avg.	1.26	1.27	1.36	1.22	2.83	2.90	2.90	10.74
σ	0.02	0.03	0.03	0.02	0.03	0.03	0.02	0.05
A-RNA [r(GC)]$_2$								
G1·C3	1.18	1.29	1.29	1.21	2.98	3.01	2.93	10.76
B-DNA [d(CCAACGTTGG)]$_2$								
Max.	1.25	1.36	1.36	1.24	2.91	2.93	2.85	10.65
Min.	1.21	1.34	1.30	1.23	2.85	2.88	2.76	10.59
Avg.	1.23	1.35	1.33	1.23	2.87	2.91	2.80	10.63
σ	0.02	0.01	0.03	0.01	0.03	0.02	0.04	0.03

Maximum, minimum, and average lengths of selected distances (in Å) for G·C base pairs. A-RNA and B-DNA duplexes adopt crystallographic twofold symmetry.

substitution at the pyrimidine 5-position on Z-DNA stability, observed in both solution and solid state. In our model, the Z-DNA destabilizing effect of A·T incorporation can be explained by partial (*in-alteration* incorporation) or complete disruption (*out-of-alteration* incorporation) of the described stabilizing interactions of O4′. The stronger stabilizing effect of C5 bromination as compared to C5 methylation can be explained by an additional strengthening of the cytidine C6—H6···O4′ hydrogen bond with the former substituent. However, the strongest support for our model comes from the Z-DNA typical coordination of various cations to O6 and N7 of guanine, as well as from the close proximity of negatively charged phosphate groups to N2 (water-mediated) and C8, which stabilize the proposed polarization of the guanine base. Such a coordination mode is rarely observed with B-DNA because of the reduced accessibility of base functions at the floor of the major groove in B-DNA compared with Z-DNA but possibly also because of differing electronic states of guanine in the two conformational environments. The suggested role of cytidine O4′ provides a plausible argument for the facilitated adoption of the left-handed Z conformation with alternating dG-dC sequences and sheds light on differences in ion coordination and hydration between Z-DNA and B-DNA. It has recently been demonstrated that the anomeric effect plays a significant role in shaping the pseudorotational potential of nucleotides (35). Inclusion of parameters for the O4′—C1′—N anomeric effect in molecular mechanics calculations led to improved correspondence with experimental data. We conclude that the stabilizing interactions described here have to be taken into account when calculating the energetic consequences of the B-DNA → Z-DNA transition and the incorporation of A·T base pairs into alternating dG-dC stretches.

1. Szarek, W. A. & Horton, D., eds. (1979) *Anomeric Effect: Origin and Consequences* (Am. Chem. Soc., Washington, DC).
2. Deslongchamps, P. (1983) *Stereoelectronic Effects in Organic Chemistry,* Tetrahedron Organic Chemistry Series (Pergamon, Oxford), Vol. 1.
3. Thatcher, G. R. J., ed. (1993) *The Anomeric Effect and Associated Stereoelectronic Effects* (Am. Chem. Soc., Washington, DC).
4. Saenger, W. (1984) *Principles of Nucleic Acid Structure* (Springer, New York).
5. Egli, M., Usman, N. & Rich, A. (1993) *Biochemistry* **32,** 3221–3237.
6. Kopka, M. L., Fratini, A. V., Drew, H. R. & Dickerson, R. E. (1983) *J. Mol. Biol.* **163,** 129–146.
7. Pjura, P. E., Grzeskowiak, K. & Dickerson, R. E. (1987) *J. Mol. Biol.* **197,** 257–271.
8. Teng, M., Usman, N., Frederick, C. A. & Wang, A. H.-J. (1988) *Nucleic Acids Res.* **16,** 2671–2690.
9. de C. T. Carrondo, M. A. A. F., Coll, M., Aymami, J., Wang, A. H.-J., van der Marel, G. A., van Boom, J. H. & Rich, A. (1989) *Biochemistry* **28,** 7849–7859.
10. Quintana, J. R., Lipanov, A. A. & Dickerson, R. E. (1991) *Biochemistry* **30,** 10294–10306.
11. Frederick, C. A., Coll, M., van der Marel, G. A., van Boom, J. H. & Wang, A. H.-J. (1988) *Biochemistry* **27,** 8350–8361.
12. Wang, A. H.-J., Quigley, G. J., Kolpak, F. J., Crawford, J. L., van Boom, J. H., van der Marel, G. A. & Rich, A. (1979) *Nature (London)* **282,** 680–686.
13. Dickerson, R. E. (1983) *Sci. Am.* **249,** 87–102.
14. Gessner, R. V., Quigley, G. J., Wang, A. H.-J., van der Marel, G. A., van Boom, J. H. & Rich, A. (1985) *Biochemistry* **24,** 237–240.
15. Gessner, R. V., Frederick, C. A., Quigley, G. J., Rich, A. & Wang, A. H.-J. (1989) *J. Biol. Chem.* **264,** 7921–7935.
16. Egli, M., Williams, L. D., Gao, Q. & Rich, A. (1991) *Biochemistry* **30,** 11388–11402.
17. Bancroft, D., Williams, L. D., Rich, A. & Egli, M. (1994) *Biochemistry* **33,** 1073–1086.
18. Gessner, R. V., Quigley, G. J. & Egli, M. (1994) *J. Mol. Biol.* **236,** 1154–1168.
19. Berman, H. M., Olson, W. K., Beveridge, D. L., Westbrook, J., Gelbin, A., Demeny, T., Hsieh, S.-H., Srinivasan, A. R. & Schneider, B. (1992) *Biophys. J.* **63,** 751–759.
20. Wing, R., Drew, H., Takano, T., Broka, C., Tanaka, S., Itakura, K. & Dickerson, R. E. (1980) *Nature (London)* **287,** 755–758.
21. Wang, A. H.-J., Hakoshima, T., van der Marel, G., van Boom, J. H. & Rich, A. (1984) *Cell* **37,** 321–331.
22. Wang, A. H.-J., Gessner, R. V., van der Marel, G. A., van Boom, J. H. & Rich, A. (1985) *Proc. Natl. Acad. Sci. USA* **82,** 3611–3615.
23. Jeffrey, G. A. & Saenger, W. (1991) *Hydrogen Bonding in Biological Structures* (Springer, New York).
24. Taylor, R. & Kennard, O. (1982) *J. Am. Chem. Soc.* **104,** 5063–5070.
25. Jeffrey, G. A., Maluszynska, H. & Mitra, J. (1985) *Int. J. Biol. Macromol.* **7,** 336–348.
26. Behe, M. & Felsenfeld, G. (1981) *Proc. Natl. Acad. Sci. USA* **78,** 1619–1623.
27. Jovin, T. M., Soumpasis, D. M. & McIntosh, L. P. (1987) *Annu. Rev. Phys. Chem.* **38,** 521–560.
28. Jovin, T. M., McIntosh, L. P., Arndt-Jovin, D. J., Zarling, D. A., Robert-Nicoud, M., van de Sande, J. H., Jorgenson, K. F. & Eckstein, F. (1983) *J. Biomol. Struct. Dyn.* **1,** 21–57.
29. Fujii, S., Wang, A. H.-J., van der Marel, G., van Boom, J. H. & Rich, A. (1982) *Nucleic Acids Res.* **10,** 7879–7892.
30. Chevrier, B., Dock, A. C., Hartmann, B., Leng, M., Moras, D., Thuong, M. T. & Westhof, E. (1986) *J. Mol. Biol.* **188,** 707–719.
31. Bürgi, H. B., Dunitz, J. D. & Shefter, E. (1973) *J. Am. Chem. Soc.* **95,** 5065–5067.
32. Bürgi, H. B., Dunitz, J. D. & Shefter, E. (1974) *Acta Crystallogr. B* **30,** 1517–1527.
33. Hoeffken, H. W., Knof, S. H., Bartlett, P. A., Huber, R., Moellering, H. & Schumacher, G. (1988) *J. Mol. Biol.* **204,** 417–433.
34. Coll, M., Knof, H., Ohga, Y., Messerschmidt, A., Huber, R., Moellering, H., Rüssmann, L. & Schumacher, G. (1990) *J. Mol. Biol.* **214,** 597–610.
35. Jalluri, R. K., Yuh, Y. H. & Taylor, E. W. (1993) in *The Anomeric Effect and Associated Stereoelectronic Effects* (Am. Chem. Soc., Washington, DC), Vol. 539, pp. 277–293.